HHS Public Access

Author manuscript

Hepatology. Author manuscript; available in PMC 2019 May 01.

Published in final edited form as:

Hepatology. 2018 May ; 67(5): 1903–1919. doi:10.1002/hep.29652.

β-catenin and IL-1β dependent CXCL10 production drives progression of disease in a mouse model of Congenital Hepatic Fibrosis

Eleanna Kaffe[1], **Romina Fiorotto**[1,2], **Francesca Pellegrino**[1], **Valeria Mariotti**[1,2,3], **Mariangela Amenduni**[1], **Massimiliano Cadamuro**[2], **Luca Fabris**[2,3], **Mario Strazzabosco**[1,2], and **Carlo Spirli**[1,2]

[1]Section of Digestive Diseases, Liver Center, Yale University, New Haven, CT, USA

[2]International Center for Digestive Health, University of Milan-Bicocca, Milan, Italy

[3]Department of Molecular Medicine, University of Padua, School of Medicine, Padua, Italy

Abstract

Congenital Hepatic Fibrosis (CHF), a genetic disease caused by mutations in the PKHD1 gene, encoding for the protein fibrocystin (FPC), is characterized by biliary dysgenesis, progressive portal fibrosis, and by a PKA-mediated activating phosphorylation of β-Catenin at Ser675. Biliary structures of *Pkhd1*$^{del4/del4}$ mice, a mouse model of CHF, secrete CXCL10 a chemokine able to recruit macrophages. The aim of this study is to clarify whether CXCL10 plays a pathogenetic role in disease progression in CHF/CD and to understand the mechanisms leading to increased CXCL10 secretion. We demonstrate that treatment of *Pkhd1*$^{del4/del4}$ mice for three-month with AMG-487, an inhibitor of CXCR3 the cognate receptor of CXCL10, reduces the peribiliary recruitment of M2 macrophages (CD45^{+}F4/80^{+} cells), spleen size, liver fibrosis (Sirius red), and cyst growth (K19^{+} area), consistent with a pathogenetic role of CXCL10. Furthermore, we show that in FPC-defective cholangiocytes, isolated from *Pkhd1*$^{del4/del4}$ mice, CXCL10 production is mediated by JAK/STAT3, in response to IL-1β and β-Catenin. Specifically, IL-1β promotes STAT3 phosphorylation whereas β-Catenin promotes its nuclear translocation. Increased pro-IL-1β was regulated by NF-kB and increased secretion of active IL-1β was mediated by the activation of NLRP3 inflammasome (increased expression of caspase 1 and NLRP33).

Conclusions—In FPC-defective cholangiocytes, β-Catenin and IL-1β are responsible for STAT3-dependent secretion of CXCL10. *In vivo* experiments show CXCL10/CXCR3 axis prevents the recruitment of macrophages, reduces inflammation and halts the progression of the disease. The increased production of IL-1β highlights the autoinflammatory nature of CHF and may open novel therapeutic avenues.

Keywords

Cholangiocytes; Fibropolycystic Liver Diseases; JAK/STAT pathway; Autoinflammatory Diseases; Macrophages

Address correspondence to: Carlo Spirli Ph.D, Section of Digestive Diseases, Liver Center, Yale University School of Medicine, Cedar Street 333, New Haven, CT 06511, USA. Phone: 203-737-6882; Fax: 203-785-7273; carlo.spirli@yale.edu.

Conflicts of interest: The authors declare that they have no competing interests.

Congenital Hepatic Fibrosis (CHF) and Caroli disease (CD) are genetic cholangiopathies caused by mutations in PKHD1, the gene encoding for fibrocystin/polyductin, a protein of unclear function, localized in the plasma membrane and cilia of cholangiocytes and renal epithelial cells (1). In CHF/CD, liver disease is characterized by cystic dysgenesia of the intrahepatic bile ducts that retain an immature phenotype (ductal plate malformations) and by portal fibrosis, leading to portal hypertension and related complications (2, 3). Portal fibrosis is the result of a complex interplay between epithelial cells, inflammatory cells and mesenchymal cells (4), ultimately leading to the activation of myofibroblasts, the effectors in the fibrotic process (2, 5–7). Exploring the factors and the mechanisms that take part in this interplay may help in discovering new therapies against portal fibrosis, a major determinant of disease progression in all cholangiopathies (4, 5).

Using the *Pkhd1*$^{del4/del4}$ mouse, an orthologous model of CHF/CD (8, 9), we previously demonstrated that increased PKA-dependent phosphorylation of β-Catenin at Ser675 promoted the nuclear translocation of transcriptionally active pSer-675-β-Catenin (10). Moreover, we have shown that in isolated fibrocystin (FPC)-defective cholangiocytes, as well as in cystic structures isolated by laser capture microdissection (LCM), the expression of chemokines and inflammatory mediators, including CXCL10 (chemokine (C-X-C motif) ligand 10) and IL-1β was increased. Furthermore, we have shown that expression of CXCL10, was β-Catenin-dependent (8).

The chemokine CXCL10, also known as interferon γ-induced protein 10 (IP-10), is a chemo-attractant for monocytes/macrophages, T cells, NK cells and dendritic cells; CXCL10 elicits its effects by binding to the cell surface receptor CXCR3 (CXC chemokine receptor family 3) (11). It has been shown that CXCL10 promotes liver fibrosis in toxin/metabolic induced liver fibrosis models and recruits inflammatory cells (12) (13) especially macrophages (14). In epithelial cells (15) CXCL10 secretion is induced by other pro-inflammatory cytokines, including IL-1β.

This study aims to clarify whether CXCL10 secretion by cholangiocytes plays a pathogenetic role in disease progression in CHF/CD and to understand the mechanisms leading to increased CXCL10 secretion. We demonstrate that *in vivo* inhibition of the CXCL10/CXCR3 axis reduces the peribiliary recruitment of M2 macrophages and slows disease progression and fibrosis. Furthermore, we show that in FPC-defective cholangiocytes, CXCL10 production is mediated by JAK/STAT3 (Janus kinase/Signal transducer and activator of transcription 3), in response to IL-1β and β-Catenin. Specifically, IL-1β is responsible for STAT3 phosphorylation whereas β-Catenin is responsible for its nuclear translocation. Increased production of IL-1β appears to be an early phenomenon in *Pkhd1*$^{del4/del4}$ mice, likely regulated by NF-kB and by the NLRP3 (Nod-like receptors, pyrin domain containing 3) inflammasome activation. These results provide novel understanding of the autoinflammatory nature of the CHF/CD and open novel opportunities for effective treatments.

MATERIAL AND METODS

Reagents

All the reagents used are listed in the supplementary material. While, all the antibodies used and relative suppliers are listed in Supplementary Table 1.

Mouse Model

Pkhd1$^{del4/del4}$ mouse is a well-established model for human CHF and ARPKD disease (8, 9) and was a kind gift from S. Somlo, Yale University, New Haven, CT. All animals were housed at the Yale Animal Care facility and animal experimental protocols were approved by the Yale Animal Care and Use Committee (IACUC) and the Office of Animal Research Support (OARS). The *Pkhd1*$^{del4/del4}$ mouse, of a mixed C57BL6/129Sv background, is a carrier for inactivating deletion in the exon 4 of the Pkhd1 gene. These mice mimic the human hepatic disease, developing cysts splenomegaly and progressive portal fibrosis in the liver as previously described (8, 9). Mice were fed a regular chow diet. Littermate, sex and age matched WT and *Pkhd1*$^{del4/del4}$ mice were treated with a small molecule CXCL10/CXCR3 antagonist, AMG-487, (5mg/Kg) (16) or with the vehicle (20% hydroxypropyl-β-cyclodextrin) orally every other day a week for 12 weeks, starting 3 months after birth. The injections were performed in the light cycle. At the end of the treatment, non-fasted mice were anesthetized by use of Ketamine (100mg/Kg) in combination with Xylazine (10mg/Kg) intraperitoneally (I.P) and sacrificed. Liver tissue (two main lobes), were harvested and fixed in formalin and then embedded in paraffin for histochemical analysis; the small liver lobes were snap frozen in liquid nitrogen. Liver slides 5 m thick were processed and stained with hematoxylin/eosin or markers for number of cysts (K19), inflammatory infiltration (CD45) and collagen deposition (Sirius red) evaluation.

Isolation and culture of Cholangiocytes—Mouse cholangiocytes were isolated from *Pkhd1*$^{del4/del4}$ and WT mice at 3 months of age as previously described (8, 10, 17–20) and detailed in the supplementary material.

Immunohistochemistry—Liver tissue sections obtained from both *Pkhd1*$^{del4/del4}$ and WT mice were deparaffinized in xylene and rehydrated in water. The staining was performed as detailed in the supplementary material.

Immunocytochemistry—Cells grown on 6-wells plates, were fixed on cold methanol for 10 minutes at −20°C. The staining was performed as detailed in the supplementary material.

PLA (Proximity Ligation Assay)—The PLA was performed as previously described (20) and detailed in the supplementary material.

Real-Time Reverse-Transcription Polymerase Chain Reaction—Total RNA was isolated from WT and FPC-defective cholangiocytes using TRIzol Reagent (Invitrogen, Carlsband, CA) per manufacturer's instructions. Briefly, 1000 ng RNA were converted into a PCR template using the Reverse Transcription Kit (Applied Biosystem) which was then used for the real-time PCR analysis using commercially available specific FAM conjugated

probes for *Cxcl-10, Cxcl-9, Cxcl-11, IL-1β, β-catenin* and *hprt* (TaqMan, Invitrogen CA) in combination with the Fast Start Universal Probe Master mix (Rox) (Roche Diagnostics, Indianapolis, IN) on an Applied Biosystems 7500 Real-Time PCR System. For Nlrp3 gene expression unconjugated probes were used (F: CGG ATG TTA TTC TGG CAA CA, R: CGC TTT GGA GAT GGA TCT GT) in combination with SYBR Green master mix (Applied Biosystems, UK). Data were normalized against the housekeeping gene (*hprt*) and analyzed using the ΔΔCt method.

Liver Cell Isolation and Fluorescence-Activated Cell Sorting Analysis— Fluorescence-activated cell sorting analysis was performed to characterize the different cell subsets contributing to the portal inflammatory cell infiltrate and to characterize the cell populations expressing pSTAT3 and CXCR3, as previously described (8, 21) and detailed in the supplementary material.

β-Catenin silencing—Pre-designed custom short-interfering RNA (siRNA) from Dharmacon were used for β-catenin silencing and detailed in the supplementary material.

Western blot

Samples of nuclear, cytoplasmic or whole-cell extracts were used for Western blot, as detailed in supplementary materials.

Statistical analysis

Results are shown as mean±SEM. Statistical comparisons were made using Student's t tests, or Mann-Whitney for non-normal distributions. ANOVA with post-hoc corrections was performed where more than two groups were compared. Statistical analyses were performed using GRAPH PAD software (SAS, Cary, NC); p values <0.05 were considered significant.

RESULTS

Inhibition of the CXCL10/CXCR3 axis *in vivo* reduces inflammation, fibrosis and cysts growth in *Pkhd1*$^{del4/del4}$ mice

Our prior studies have shown that production of CXCL10 is increased in *Pkhd1*$^{del4/del4}$ mice and FPC-defective cholangiocytes and that the secretion of CXCL10 by cystic cholangiocytes is able to recruit macrophages *in vitro* (8). We have also shown that macrophages play an important role in fibrosis progression in the *Pkhd1*$^{del4/del4}$ mice (8). Thus, we hypothesized that secreted CXCL10 may play an important role in the recruitment of macrophages and in disease progression in *Pkhd1*$^{del4/del4}$ mice *in vivo*. To test this hypothesis, we studied the effects of inhibiting the CXCR3-CXCL10 axis in *Pkhd1*$^{del4/del4}$ mice. Of note the other ligands for CXCR3, CXCL9 and CXCL11, were not significantly different in liver samples from *Pkhd1*$^{del4/del4}$ mice (Supplementary Figure 1A, C). Moreover, CXCL9 and CXCL11 secretion was not detectable in FPC-defective cholangiocytes (not shown).

Fluorescence-activated cell sorting analysis (FACS) confirmed that CXCR3, the cognate receptor for CXCL10 was expressed in cells isolated from whole livers explanted from

three-month-old mice, including fibroblasts (Collagen 1^+ Cells) (Supplementary Figure 1D, E), macrophages (F4/80^+ Cells) (Supplementary Figure 1F, G) and cholangiocytes (Cytokeratin 19^+ Cells) (Supplementary Figure 1 H, I). Thus, we treated 3-months-old *Pkhd1*$^{del4/del4}$ and WT mice with AMG-487 (5 mg/Kg orally, 4 times/week for 3 months), a small molecule antagonist of CXCR3 or with its vehicle (20% hydroxypropyl-β-cyclodextrin). The results show that inhibition of the CXCL10/CXCR3 axis significantly reduced disease progression in *Pkhd1*$^{del4/del4}$ mice, as shown by decrease in the inflammatory infiltrate (47% reduction in CD45 positive area) (Figure 1A), in the amount of Cytokeratin 19 (K19)-positive cysts (37% reduction in K19 positive area) (Figure 1B), and in pericystic collagen deposition (53% reduction in Sirius red positive area) (Figure 1C) and a reduction in splenomegaly (35% reduction in the relative spleen weight) (Figure 1E). FACS analysis of $CD45^+$ inflammatory infiltrate showed that CXCL10/CXCR3 inhibition reduced the number of macrophage ($CD45^+CD11b^+F4/80^+$) infiltration by 40% (Figure 2A, B) and of T-cells by 50% ($CD45^+CD11b^-CD4^+$) (Figure 2A, B) in the liver of *Pkhd1*$^{del4/del4}$ mice treated with AMG-487. On the other hand, the levels of other immune subpopulations such as granulocytes ($CD45^+CD11b^+F4/80^-Gr1^+$), Natural Killer (NK) cells ($CD45^+CD11b^{hi-}NK1.1^+$), CD8 ($CD45^+CD11b^-CD8^+$) and B cells ($CD45^+CD11b^-CD19^+$), remained unchanged or slightly reduced upon CXCR3 inhibition (Figure 2B).

Our previous studies have shown that in *Pkhd1*$^{del4/del4}$ mice the M1/M2 ratio decreases gradually from 1 month to 12 months of age because of a progressive increase of M2 polarized macrophages and that the increase in M2 macrophages correlated with fibrosis and splenomegaly (8). In the present study, we show that after CXCR3 inhibition, the M2 subtype of macrophages ($CD45^+F4/80^+Erg2^+$) (22) decreased by 60% (Figure 2C, D), while the M1 ($CD45^+F4/80^+NOS2^+$) subtype slightly increases (Figure 2C, D). These changes resulted in an increased M1/M2 ratio (Figure 2E). The decrease in M2 polarized macrophages after CXCR3 antagonism correlated with the reduced pericystic collagen deposition observed in the same mice (Figure 1C). These data suggest that CXCL10/CXCR3 axis plays an important role in macrophages recruitment in CHD/CD and a pathophysiological role in disease progression. Therefore, we deemed important to better understand the mechanisms leading to increased CXCL10 secretion in FPC-defective cholangiocytes.

β-Catenin stimulates CXCL10 secretion by promoting the nuclear translocation of pSTAT3 in FPC-defective cholangiocytes

As CXCL10 is regulated by the JAK/STATs pathway, we tested the expression and the phosphorylation status of different STATs isoforms by FACS analysis of whole liver cell extracts and in isolated cells. We found that in three-months old *Pkhd1*$^{del4/del4}$ mice, only STAT3, phosphorylated at Tyr705, was significantly increased in the $K19^+$ cell fraction (Figure 3A–B). pSTAT3(Tyr705) is known to translocate into the nucleus and to activate the transcription of several genes (23). The increased expression of pSTAT3 in the cystic epithelium in *Pkhd1*$^{del4/del4}$ mice was further confirmed by immunohistochemistry of mouse liver specimens (Supplementary Figure 2A, B). Increased pSTAT3 was also observed *in vitro,* in cultured cholangiocytes by immunofluorescence (IF), FACS and Western blot. In fact, pSTAT3 was expressed in FPC-defective cholangiocytes at higher levels as compared to

WT cells (Figure 3C, D, Figure 5E, F). In addition, treatment for 24 hours using a JAK inhibitor (pan-JAK inhibitor, 10 μM), or a STAT3 inhibitor (Static V, 10 μM) significantly reduced CXCL10 gene expression and secretion (Figure 3E, F). CXCL10 gene and protein expression decreased by 50% when treated with the STAT3 inhibitor (Figure 3E, F) and by 80% (gene level) and 40% (protein level) with the JAK inhibitor (Figure 3E, F) in FPC-defective cholangiocytes. On the contrary, in WT cells, CXCL10 was inhibited only by the JAK inhibitor and only at gene level (Figure 3E).

We have previously shown that inhibition of β-Catenin by ICG-001 or by Quercetin reduced CXCL10 production in FPC-defective cholangiocytes (8). To further confirm the β-Catenin-dependence of CXCL10 production, we silenced β-Catenin in WT and FPC-defective cholangiocytes, using specific siRNAs, that achieved a considerable reduction of β-Catenin (60% at mRNA and by 65% at the protein levels 48 hours post transfection) (Figure 4A, B). Beta-Catenin silencing significantly reduced CXCL10 both at the mRNA level (80% reduction) (Figure 4C) as well as at the secreted protein level (50% reduction) in FPC-defective cholangiocytes, (Figure 4D). Interestingly, among the different STATs (STAT1, STAT3 and STAT5) only STAT3 was β-Catenin dependent (Supplementary Figure 5 A, B).

Moreover, in agreement with our previous data showing that the cAMP/PKA pathway activates β-catenin in FPC-defective cholangiocytes, we found that increasing cAMP levels induced CXCL10 gene expression and protein secretion and this was abolished upon PKA inhibition (Figure 4E, F). Interestingly, the cAMP and β-catenin dependence of CXCL10 production was only evident in FPC-defective cholangiocytes, as WT cholangiocytes were not affected, indicating that these changes may be directly related to the fibrocystin function.

Having established that STAT3 and β-Catenin control CXCL10 production in FPC-defective cholangiocytes, we investigated if STAT3 phosphorylation was affected by β-Catenin silencing. As shown in Figure 5, we found that β-Catenin silencing did not change the amount of total STAT3, but reduced the nuclear fraction of pSTAT3 in FPC-defective cholangiocytes (Figure 5A–D, Supplementary Figure 3C). The same results were obtained by using the β-Catenin inhibitor ICG-001 (10 μM, one-hour treatment) (Figure 5, E, F, Supplementary Figure 3A). This effect was specific for FPC-defective cholangiocytes, as it was not observed in WT cells. (Figure 5, E, F, Supplementary Figure 3A, B). Furthermore, we found that inhibition of Rac1 significantly reduced the amount of nuclear pSTAT3 (Figure 5E). Finally, by using the PLA assay, we also show evidence (figure 5F) that β-catenin and STA3 physically interact. These important results are in agreement with our previous finding (10) showing that Rac1 facilitated β-catenin nuclear translocation in FPC^{-} cholangiocytes, and with other studies (24) showing that Rac1 is required for STAT3 nuclear translocation. Thus, altogether our data suggest that STA3 and β-catenin bind together and Rac1 facilitate the nuclear translocation of this complex.

Increased IL-1β stimulates CXCL10 secretion through STAT3 in FPC-defective cholangiocytes

We have previously showed that, pro-IL-1β gene is over-expressed by liver cysts isolated with LCM in *Pkhd1*$^{del4/del4}$ mice (8). Consistent with these observations, we found that *in vivo,* the gene expression of *pro-IL-1β* precedes the expression of C*xcl10*. In fact, in FACS-

sorted EpCAM-positive isolated cholangiocytes, at one month of age, *pro-IL-1β* gene expression levels were already significantly increased (Figure 6A), on the contrary to *Cxcl10* which expression was not increased at the same age (Figure 6B). IF of liver specimens showed that FPC-defective cholangiocytes expressed IL-1β at the cell surface (Figure 6C, Supplementary Figure 4A) already at one month of age, whereas CXCL10 expression was not detected at one month of age, (Supplementary Figure 4A). Whereas, CXCL10 was clearly detected at 3 months of age (Supplementary Figure 4A).

We next measured pro-IL-1β gene expression and secretion in the supernatant of cultured FPC-defective cholangiocytes and found that both pro-IL1β mRNA and IL-1β were significantly increased (Figure 7A, B). Secretion of IL-1β by isolated FPC-defective cells indicate this is a cell-autonomous phenomenon, possibly a consequence of defective fibrocystin.

Since IL-1β, is known to induce the production of several chemokines (25), we tested the hypothesis that IL-1β may modulate CXCL10 expression in FPC-defective cholangiocytes. After treating WT and FPC-defective cholangiocytes with IL-1β (5 ng/ml) for 24 hours we found that IL-1β increased *Cxcl10* gene expression by 16-fold (RT-PCR) and CXCL10 protein secretion by two-fold (ELISA) in FPC-defective cholangiocytes but not in WT cells (Figure 7C, D).

To understand if IL-1β induces CXCL10 secretion in FPC-defective cholangiocytes via STATs we treated the cells with IL-1β alone or in combination with STAT1, STAT3, STAT5 inhibitors for 24 hours. We found that only STAT3 inhibition (10 μM, Static-V) resulted in 90% reduction of IL-1β-induced CXCL10 expression at the gene level and 40% reduction at protein level (Figure 7C, D, Supplementary Figure 5C). Furthermore, treatment with IL-1β increased STAT3 phosphorylation in FPC-defective cholangiocytes (Figure 7E). While, treatment with IL-1β together with JAK and Tyk2 inhibitor results in a complete deletion of pSTAT3 phosphorylation (Figure 7F). Altogether, these data indicate that IL-1β and β-Catenin cooperate in increasing CXCL10 production by significantly activating the JAK/pSTAT3 pathway and by mediating its nuclear translocation.

Pro-IL-1β expression and IL-1β secretion in *Pkhd1*$^{del4/del4}$ mice are controlled by NF-kB and NLRP3 inflammasome activation, respectively

IL-1β is produced as pro-IL1β, and needs specific enzymatic cleavage to become active (26). Therefore, we tested if the main factors involved in IL-1β gene expression (NF-kB) and protein secretion (Inflammasome) were upregulated in FPC-defective cholangiocytes. Expression of nuclear NF-kB phosphorylated p65 at Ser276 and Ser536, as assessed by IF and by Western blot of the nuclear fraction of cell lysates, was increased in FPC-defective cholangiocytes as compared to WT cells (Supplementary Figure 6A, Figure 8A). These phosphorylation sites are known to increase the binding of NF-kB to DNA (Ser276) and the transcriptional activity of NF-kB (Ser536) (27). In fact, in FPC-defective cells NF-kB transcriptional activity was higher compared to WT cells (Supplementary Figure 6B). NF-kB inhibition resulted in 60% reduction of IL-1β gene expression in FPC-defective cholangiocytes (Supplementary Figure 6C) and in 50% reduction in the IL-1β secretion (Supplementary Figure 6D). Interestingly, the increased NF-kB transcriptional activity in the

isolated cells was β-Catenin (Supplementary Figure 6E) and STAT3 dependent (Supplementary Figure 6F) as shown the 50% reduction in NF-kB transcriptional activity caused by silencing the β-Catenin or by 80% reduction upon STAT3 inhibition in FPC-defective cholangiocytes. The decrease of NF-kB transcriptional activity upon β-catenin silencing was shown also for IL-1β because under these conditions, a 40% reduction in IL-1β gene expression and secretion was observed (Supplementary Figure 6G, H). Altogether, these data suggest that β-Catenin regulates CXCL10 production by acting on the nuclear import of pSTAT3 and by increasing IL-1β gene expression through NF-kB.

Furthermore, we demonstrated a two-fold increase in cleaved caspase-1 protein levels *in* FPC- defective cholangiocytes in total lysate (Figure 8B) and a fourfold increase in the *Nlrp3* gene expression (Figure 8C) as compared to WT cholangiocytes. In addition, MCC950 10 μM, an inhibitor of the NLRP3 inflammasome caused a significant reduction (40%) in IL-1β secretion in FPC-defective but not in WT cholangiocytes (Figure 8D). Altogether, these data strongly indicate that both NF-kB and the NLRP3 inflammasome are activated leading to increased bioactive IL-1β in FPC-defective cholangiocytes.

DISCUSSION

The major findings of this study are: a) blockage of CXCR3, the receptor of CXCL10, slows disease progression in the FPC defective model of CHF/CD by reducing the recruitment of macrophages, collagen deposition and cysts expansion; b) CXCL10 production is mediated by JAK/STAT3, IL-1β, and the β-Catenin pathways; c) β-Catenin is responsible for pSTAT3 nuclear translocation, whereas IL-1β is responsible for JAK/STAT3 phosphorylation; d) pro-IL-1β is regulated by β-Catenin-dependent NF-kB stimulation, whereas increased NLRP3 inflammasome activity regulates IL-1β production. Understanding the mechanistic relationships between biliary dysfunction and portal fibrosis (4), can be beneficial for the development of more effective therapies.

We have recently shown by laser capture microscopy (LCM) that in *Pkhd1*$^{del4/del4}$ mouse, cystic cholangiocytes produce cytokines, such as IL-1β, and several chemokines (including MCP-1, CXCL1, CXCL5, CXCL10, CXCL12) that are able to recruit macrophages (8) and may play an important role in the cross talk of cholangiocytes with inflammatory and mesenchymal cell types that drive the progression of the disease (4). In the *Pkhd1*$^{del4/del4}$ mouse (8) the phenotype of infiltrating macrophages progressively change due to an increase in M2 macrophages; this is associated with increased production of TGF-β, and other growth factors that promote proliferation of collagen producing cells, and extracellular matrix deposition (28). Clarification of these mechanisms may lead to a better understanding of the molecular events that link the epithelial dysfunction with inflammation and fibrosis. Among them, we focused on CXCL10 because of its reported role in inflammation and fibrosis in other liver diseases (11).

To investigate if CXCL10 plays a pathogenetic role in disease progression *in vivo*, we studied if inhibition of the CXCR3-CXCL10 axis could block macrophage recruitment. Of note, CXCL9 and CXCL11, the other CXCR3 ligands were not upregulated in liver samples from *Pkhd1*$^{del4/del4}$ mice. Indeed, inhibition of CXCR3 *in vivo* for 3 months (AMG-487)

reduced $CD45^{+}$ immune cells infiltration and collagen deposition, thereby slowing the progression of the disease. Furthermore, treatment with AMG-487 modified the M1/M2 ratio by reducing the amount of M2 macrophages. Moreover, besides the M2 reduction, CXCR3 inhibition reduced also the number of total macrophages (especially the infiltrating ones that are $F4/80^{low}$ $CD11^{high}$) and T-cells that are pro-inflammatory. Thus, the benefit of reducing a significant number of inflammatory cells outweigh the disadvantage of reducing an anti-inflammatory population (M2). The reduced fibrosis and inflammation were accompanied by a significant reduction in splenomegaly and in liver cysts. The improvement in fibrosis and liver cysts, after CXCR3 blockade, is consistent with the reduced disease progression reported after depletion of macrophages with liposomal clodronate (8). Furthermore, given the expression of CXCR3 in cholangiocytes, fibroblasts and macrophages, it is likely that in our model all these cell populations respond to CXCL10, secreted by cholangiocytes and immune cells once attracted around the dysmorphic bile ducts.

Having established that CXCL10 has a major pathogenetic role in CHF, we further investigated the mechanism regulating its production by cholangiocytes. We have previously shown that CXCL10 production by FPC-defective cholangiocytes was inhibited by chemical inhibition of β-catenin signaling (8). To confirm this result, we silenced β-catenin and found that CXCL10 gene expression and secretion were diminished. Interestingly, this effect was specific for FPC-defective cells, as no changes in CXCL10 secretion were found in β-catenin-silenced WT cells. Moreover, increasing cAMP levels induced CXCL10 gene expression and protein secretion was abolished upon PKA inhibition. The cAMP/PKA pathway was previously shown to activate β-Catenin in FPC Cholangiocytes (10). Therefore, the effect of cAMP on CXCL10 are likely mediated by β-Catenin.

To better understand the mechanisms through which β-catenin mediates CXCL10 production, we tested its relationship with other transcription factors that are known *in vitro* to be involved in CXCL10 production such as STATs (29). Among the different STATs we tested (STAT1, STAT3 and STAT5), we found that phosphorylated STAT3 was increased in the nucleus of FPC-defective cholangiocytes as compared to WT. Inhibition of β-catenin or silencings blocked only pSTAT3 nuclear translocation, but the total level of STAT3 were not affected, indicating that β-catenin mediates the nuclear translocation of pSTAT3. The role of β-Catenin in stimulating the nuclear translocation of pSTAT3 appears to be specific for FPC-defective cells. Interestingly, our data show that inhibition of Rac1 significantly reduced the amount of nuclear pSTAT3. Furthermore, by using the PLA assay, we also show evidence that β-catenin and STA3 physically interact. These important results are in agreement with our previous findings (10)showing that Rac1 facilitated β-catenin nuclear translocation in FPC-defective cholangiocytes, and with other studies (24) showing that Rac1 is required for STAT3 nuclear translocation. Thus, altogether our data suggest that STA3 and β-catenin bind together and the nuclear translocation of this complex is facilitated by Rac1.

IL-1β emerged an important player in CXCL10 production in FPC-defective cholangiocytes. IL-1β has been reported to stimulate CXCL10 in several cell types such as neural progenitor cells (25), human astrocytes (30), interstitial epithelial cells (15) and in rat islets and β cell lines (31). In FPC-defective cholangiocytes, we have found that CXCL10 induction by

IL-1β is abolished in the presence of JAK and STAT3 inhibition and that IL-1β directly induced STAT3 phosphorylation, a necessary step for STAT3 binding to specific DNA target sites (32). Thus, in aggregate our results indicate that CXCL10 is controlled by pSTAT3 and that STAT3 is regulated by both IL-1β (phosphorylation) and β-Catenin (nuclear translocation).

IL-1β needs to be bio-activated to be secreted (26). Its production and secretion require a two-step process which involves the production of pro-IL-1β, induced by NF-kB and the processing of pro-IL-1β and its enzymatic cleavage into its bioactive form mediated by specific proteases such as cysteine protease caspase-1, serine proteinases and matrix metalloproteinases (MMP) (33). The most relevant signal 2 reported in the liver disease include adenosine triphosphate (ATP), uric acid, palmitic acid, cholesterol crystals, free fatty acids, glucose, reactive oxygen species, mitochondrial stress, K^+ and Ca^{2+} content of the cell, ER stress and bacterial derived products (34).

We found that NF-kB activity is increased in FPC-defective cholangiocytes and is responsible for increased pro-IL-1β gene expression. Specifically, FPC-defective cholangiocytes showed increased levels of p65 phosphorylated at Ser276 and Ser536 as compared to WT cells. The phosphorylation of Ser276, which leads to p65 acetylation at K310 and mediates the interaction with CBP/p300, is known to be mediated by PKA (35). On the other hand, Ser536 phosphorylation leads to binding of NF-kB on TATA-binding protein-associated factor II31, a component of Transcription factor II D (TFIID) (36). Both phosphorylations enhance the transcriptional activity of NF-kB (27) consistent with our observed increased expression of NF-kB target genes such as IL-1β in FPC-defective cells. Several studies show that β-Catenin can interact with NF-kB. The positive regulation of NF-kB by β-Catenin was shown in epithelial cells (37), (38) and this may be regulated by different mechanisms. In fact, the activation of NF-kB from β-Catenin was reported to be mediated by other factors such as the presence of IL-1β that can induce a transcriptional cooperation between NF-kB and β-Catenin (39) or the loss of E-cadherin that can lead to cytoplasmic β-catenin accumulation that triggers p38-mediated NF-κB activation (40). In FPC-defective cholangiocytes, we have previously shown that E-cadherin expression is reduced (10). Moreover, several studies have shown a direct interaction of NF-kB with STAT3. In fact, STAT3 may act as trans-activators capable of recruiting p300/CREB-binding protein (CBP) and to have a critical role in retaining NF-κB in the nucleus (32) (41). Our data show that pSTAT3 inhibition reduces NF-kB transcriptional activity suggesting that β-catenin regulates NFkB activity through pSTAT3.

The intracellular cysteine protease caspase-1, a member of multimeric protein platforms called inflammasome is the most important protease for IL-1β bio-activation. In response to danger signals, inflammasomes are assembled from self-oligomerizing scaffold proteins via NACHT domain interactions. The scaffold proteins include the sensor proteins such as NLRP3 and the adaptor apoptosis-associated speck-like protein (ASC), and the pro-caspase-1. These high molecular mass complexes trigger caspase-1 autoactivation (42). Activated caspase-1 initiates the maturation of pro-IL-1β and pro-IL-18(43). The increased expression/secretion of active IL-1β by FPC-defective cholangiocytes *in vivo* and *in vitro* indicates that in our cells the inflammasome is activated. In fact, our results show and

increased expression of NLRP3 and cleaved caspase-1. The presence of an active IL-1β is of high significance because of its ability to induce an inflammatory loop, and thus sustain a vicious cycle of inflammatory responses (44). This phenomenon is at the basis of the so called autoinflammatory diseases (45), caused by either abnormal production of IL-1β due to NLRP3 mutation or deficient antagonism of IL-1β receptor. IL-1β is the major driver of these diseases and has the potential to cause both systemic and organ-specific immunopathology (44). Of note, aberrant inflammasome activation has been reported in liver diseases where it has been associated to liver damage, steatosis, inflammation and fibrosis (43, 46). Depending on the cell type, IL-1β mediates the release of chemokines, cytokines, inflammatory mediators, including TNF-α, CXCL-10, IL-8, inducible nitric oxide synthase, COX-2, prostaglandin E2, nitric oxide and type 2 phospholipase A (45). It is important to note, that IL-1β can be active even at very low concentration such as 2–10 pg/ml (47). Thus, the early production of IL-1β may play an important role in macrophages recruitment at early disease stage directly or indirectly through the production of other chemo-attractants such as CXCL10.

In conclusion, our results indicate that in FPC-defective cholangiocytes, CXCL10 production is mediated by JAK/STAT3; β-Catenin is responsible for pSTAT3 nuclear translocation, whereas IL-1β is responsible for STAT3 phosphorylation. Furthermore, we found that β-Catenin controls NF-kB transcriptional activity which together with the NLRP3 inflammasome regulates IL-1β production. Finally, inhibition of CXCR3, the cognate receptor for CXCL10, halts the progression of the disease by reducing fibrosis and splenomegaly and the recruitment of M2 macrophages. These results highlights CHF as an autoinflammatory disease and may open new therapeutic avenue.

Supplementary Material

Refer to Web version on PubMed Central for supplementary material.

Acknowledgments

Funding: This work was funded by the National Institute of Diabetes and Digestive and Kidney Diseases of the National Institutes of Health under Award Number RO1DK101528 to CS, P30 DK034989-Silvio O. Conte Digestive Diseases Research Core Center to CS, MS and RF and by RO1 DK079005 to MS.

List of abbreviations

CHF	Congenital Hepatic Fibrosis
FPC	fibrocystin
CD	Caroli disease
PKA	Protein kinase A
CXCL10	chemokine (C-X-C motif) ligand 10
CXCR3	CXC chemokine receptor family 3
JAK/STAT3	Janus kinase/Signal transducer and activator of transcription 3

NF-kB	nuclear factor kappa-light-chain-enhancer of activated B cells
NLRP3	Nod-like receptors, pyrin domain containing 3
RT-PCR	Reverse transcription polymerase chain reaction
ELISA	Enzyme-linked Immunosorbent Assay
FACS	Fluorescence-activated cell sorting
K19	Cytokeratin 19
NK	Natural Killer
M1	classical activated macrophages
M2	alternative activated macrophages
NOS2	Nitric Oxide synthase-2
Erg-2	Early growth response protein 2
IF	Immunofluorescence
MCP-1	Monocyte chemoattractant protein-1
TGF-β	Transforming growth factor beta
NASH	Non Alcoholic Steatohepatitis
PBC	Primary biliary cholangitis
MMP	matrix metalloproteinases
ASC	adaptor apoptosis-associated speck-like protein
ATP	adenosine triphosphate
TNF-α	Tumor necrosis factor a
COX-2	Cyclooxygenase-2
Pan-Akt	pan-protein kinase isoforms 1,2,3

References

Author names in bold designate shared co-first authorship.

1. Harris PC, Torres VE. Polycystic kidney disease. Annu Rev Med. 2009; 60:321–337. [PubMed: 18947299]
2. Strazzabosco M, Somlo S. Polycystic liver diseases: congenital disorders of cholangiocyte signaling. Gastroenterology. 2011; 140:1855–1859. 1859e1851. [PubMed: 21515270]
3. Strazzabosco M, Fabris L. Development of the bile ducts: essentials for the clinical hepatologist. J Hepatol. 2012; 56:1159–1170. [PubMed: 22245898]
4. Fabris L, Strazzabosco M. Epithelial-mesenchymal interactions in biliary diseases. Semin Liver Dis. 2011; 31:11–32. [PubMed: 21344348]

5. Strazzabosco M, Fabris L, Spirli C. Pathophysiology of cholangiopathies. J Clin Gastroenterol. 2005; 39:S90–S102. [PubMed: 15758666]
6. Lazaridis KN, Strazzabosco M, Larusso NF. The cholangiopathies: disorders of biliary epithelia. Gastroenterology. 2004; 127:1565–1577. [PubMed: 15521023]
7. Strazzabosco M, Spirli C, Okolicsanyi L. Pathophysiology of the intrahepatic biliary epithelium. J Gastroenterol Hepatol. 2000; 15:244–253. [PubMed: 10764023]
8. Locatelli L, Cadamuro M, Spirli C, Fiorotto R, Lecchi S, Morell CM, Popov Y, et al. Macrophage recruitment by fibrocystin-defective biliary epithelial cells promotes portal fibrosis in congenital hepatic fibrosis. Hepatology. 2016; 63:965–982. [PubMed: 26645994]
9. Gallagher AR, Esquivel EL, Briere TS, Tian X, Mitobe M, Menezes LF, Markowitz GS, et al. Biliary and pancreatic dysgenesis in mice harboring a mutation in Pkhd1. Am J Pathol. 2008; 172:417–429. [PubMed: 18202188]
10. Spirli C, Locatelli L, Morell CM, Fiorotto R, Morton SD, Cadamuro M, Fabris L, et al. Protein kinase A-dependent pSer(675) -beta-catenin, a novel signaling defect in a mouse model of congenital hepatic fibrosis. Hepatology. 2013; 58:1713–1723. [PubMed: 23744610]
11. Marra F, Tacke F. Roles for chemokines in liver disease. Gastroenterology. 2014; 147:577–594. e571. [PubMed: 25066692]
12. Hintermann E, Bayer M, Pfeilschifter JM, Luster AD, Christen U. CXCL10 promotes liver fibrosis by prevention of NK cell mediated hepatic stellate cell inactivation. J Autoimmun. 2010; 35:424–435. [PubMed: 20932719]
13. Zhang X, Shen J, Man K, Chu ES, Yau TO, Sung JC, Go MY, et al. CXCL10 plays a key role as an inflammatory mediator and a non-invasive biomarker of non-alcoholic steatohepatitis. J Hepatol. 2014; 61:1365–1375. [PubMed: 25048951]
14. Tomita K, Freeman BL, Bronk SF, LeBrasseur NK, White TA, Hirsova P, Ibrahim SH. CXCL10-Mediates Macrophage, but not Other Innate Immune Cells-Associated Inflammation in Murine Nonalcoholic Steatohepatitis. Sci Rep. 2016; 6:28786. [PubMed: 27349927]
15. Yeruva S, Ramadori G, Raddatz D. NF-kappaB-dependent synergistic regulation of CXCL10 gene expression by IL-1beta and IFN-gamma in human intestinal epithelial cell lines. Int J Colorectal Dis. 2008; 23:305–317. [PubMed: 18046562]
16. Walser TC, Rifat S, Ma X, Kundu N, Ward C, Goloubeva O, Johnson MG, et al. Antagonism of CXCR3 inhibits lung metastasis in a murine model of metastatic breast cancer. Cancer Res. 2006; 66:7701–7707. [PubMed: 16885372]
17. Spirli C, Okolicsanyi S, Fiorotto R, Fabris L, Cadamuro M, Lecchi S, Tian X, et al. ERK1/2-dependent vascular endothelial growth factor signaling sustains cyst growth in polycystin-2 defective mice. Gastroenterology. 2010; 138:360–371. e367. [PubMed: 19766642]
18. Fiorotto R, Villani A, Kourtidis A, Scirpo R, Amenduni M, Geibel PJ, Cadamuro M, et al. The cystic fibrosis transmembrane conductance regulator controls biliary epithelial inflammation and permeability by regulating Src tyrosine kinase activity. Hepatology. 2016; 64:2118–2134. [PubMed: 27629435]
19. Spirli C, Villani A, Mariotti V, Fabris L, Fiorotto R, Strazzabosco M. Posttranslational regulation of polycystin-2 protein expression as a novel mechanism of cholangiocyte reaction and repair from biliary damage. Hepatology. 2015; 62:1828–1839. [PubMed: 26313562]
20. Spirli C, Mariotti V, Villani A, Fabris L, Fiorotto R, Strazzabosco M. Adenylyl cyclase 5 links changes in calcium homeostasis to cAMP-dependent cyst growth in polycystic liver disease. J Hepatol. 2017; 66:571–580. [PubMed: 27826057]
21. Yu YR, O'Koren EG, Hotten DF, Kan MJ, Kopin D, Nelson ER, Que L, et al. A Protocol for the Comprehensive Flow Cytometric Analysis of Immune Cells in Normal and Inflamed Murine Non-Lymphoid Tissues. PLoS One. 2016; 11:e0150606. [PubMed: 26938654]
22. Jablonski KA, Amici SA, Webb LM, de Ruiz-Rosado JD, Popovich PG, Partida-Sanchez S, Guerau-de-Arellano M. Novel Markers to Delineate Murine M1 and M2 Macrophages. PLoS One. 2015; 10:e0145342. [PubMed: 26699615]
23. Levy DE, Lee CK. What does Stat3 do? J Clin Invest. 2002; 109:1143–1148. [PubMed: 11994402]
24. Simon AR, Vikis HG, Stewart S, Fanburg BL, Cochran BH, Guan KL. Regulation of STAT3 by direct binding to the Rac1 GTPase. Science. 2000; 290:144–147. [PubMed: 11021801]

25. Pugazhenthi S, Zhang Y, Bouchard R, Mahaffey G. Induction of an inflammatory loop by interleukin-1beta and tumor necrosis factor-alpha involves NF-kB and STAT-1 in differentiated human neuroprogenitor cells. PLoS One. 2013; 8:e69585. [PubMed: 23922745]
26. Lamkanfi M, Dixit VM. Mechanisms and functions of inflammasomes. Cell. 2014; 157:1013–1022. [PubMed: 24855941]
27. Chen LF, Williams SA, Mu Y, Nakano H, Duerr JM, Buckbinder L, Greene WC. NF-kappaB RelA phosphorylation regulates RelA acetylation. Mol Cell Biol. 2005; 25:7966–7975. [PubMed: 16135789]
28. Ju C, Tacke F. Hepatic macrophages in homeostasis and liver diseases: from pathogenesis to novel therapeutic strategies. Cell Mol Immunol. 2016; 13:316–327. [PubMed: 26908374]
29. Clarke DL, Clifford RL, Jindarat S, Proud D, Pang L, Belvisi M, Knox AJ. TNFalpha and IFNgamma synergistically enhance transcriptional activation of CXCL10 in human airway smooth muscle cells via STAT-1, NF-kappaB, and the transcriptional coactivator CREB-binding protein. J Biol Chem. 2010; 285:29101–29110. [PubMed: 20833730]
30. Oh JW, Schwiebert LM, Benveniste EN. Cytokine regulation of CC and CXC chemokine expression by human astrocytes. J Neurovirol. 1999; 5:82–94. [PubMed: 10190694]
31. Burke SJ, Goff MR, Lu D, Proud D, Karlstad MD, Collier JJ. Synergistic expression of the CXCL10 gene in response to IL-1beta and IFN-gamma involves NF-kappaB, phosphorylation of STAT1 at Tyr701, and acetylation of histones H3 and H4. J Immunol. 2013; 191:323–336. [PubMed: 23740952]
32. Yu Z, Zhang W, Kone BC. Signal transducers and activators of transcription 3 (STAT3) inhibits transcription of the inducible nitric oxide synthase gene by interacting with nuclear factor kappaB. Biochem J. 2002; 367:97–105. [PubMed: 12057007]
33. van de Veerdonk FL, Netea MG, Dinarello CA, Joosten LA. Inflammasome activation and IL-1beta and IL-18 processing during infection. Trends Immunol. 2011; 32:110–116. [PubMed: 21333600]
34. Latz E, Xiao TS, Stutz A. Activation and regulation of the inflammasomes. Nat Rev Immunol. 2013; 13:397–411. [PubMed: 23702978]
35. Wang P, Zhu F, Lee NH, Konstantopoulos K. Shear-induced interleukin-6 synthesis in chondrocytes: roles of E prostanoid (EP) 2 and EP3 in cAMP/protein kinase A- and PI3-K/Akt-dependent NF-kappaB activation. J Biol Chem. 2010; 285:24793–24804. [PubMed: 20516073]
36. Buss H, Dorrie A, Schmitz ML, Hoffmann E, Resch K, Kracht M. Constitutive and interleukin-1-inducible phosphorylation of p65 NF-{kappa}B at serine 536 is mediated by multiple protein kinases including I{kappa}B kinase (IKK)-{alpha}, IKK{beta}, IKK{epsilon}, TRAF family member-associated (TANK)-binding kinase 1 (TBK1), and an unknown kinase and couples p65 to TATA-binding protein-associated factor II31-mediated interleukin-8 transcription. J Biol Chem. 2004; 279:55633–55643. [PubMed: 15489227]
37. Jang J, Ha JH, Chung SI, Yoon Y. Beta-catenin regulates NF-kappaB activity and inflammatory cytokine expression in bronchial epithelial cells treated with lipopolysaccharide. Int J Mol Med. 2014; 34:632–638. [PubMed: 24938929]
38. Anson M, Crain-Denoyelle AM, Baud V, Chereau F, Gougelet A, Terris B, Yamagoe S, et al. Oncogenic beta-catenin triggers an inflammatory response that determines the aggressiveness of hepatocellular carcinoma in mice. J Clin Invest. 2012; 122:586–599. [PubMed: 22251704]
39. Yun K, So JS, Jash A, Im SH. Lymphoid enhancer binding factor 1 regulates transcription through gene looping. J Immunol. 2009; 183:5129–5137. [PubMed: 19783677]
40. Solanas G, Porta-de-la-Riva M, Agusti C, Casagolda D, Sanchez-Aguilera F, Larriba MJ, Pons F, et al. E-cadherin controls beta-catenin and NF-kappaB transcriptional activity in mesenchymal gene expression. J Cell Sci. 2008; 121:2224–2234. [PubMed: 18565826]
41. Yang J, Liao X, Agarwal MK, Barnes L, Auron PE, Stark GR. Unphosphorylated STAT3 accumulates in response to IL-6 and activates transcription by binding to NFkappaB. Genes Dev. 2007; 21:1396–1408. [PubMed: 17510282]
42. Schroder K, Tschopp J. The inflammasomes. Cell. 2010; 140:821–832. [PubMed: 20303873]
43. Szabo G, Csak T. Inflammasomes in liver diseases. J Hepatol. 2012; 57:642–654. [PubMed: 22634126]

44. Dinarello CA. Immunological and inflammatory functions of the interleukin-1 family. Annu Rev Immunol. 2009; 27:519–550. [PubMed: 19302047]

45. de Jesus AA, Canna SW, Liu Y, Goldbach-Mansky R. Molecular mechanisms in genetically defined autoinflammatory diseases: disorders of amplified danger signaling. Annu Rev Immunol. 2015; 33:823–874. [PubMed: 25706096]

46. Kubes P, Mehal WZ. Sterile inflammation in the liver. Gastroenterology. 2012; 143:1158–1172. [PubMed: 22982943]

47. Petrasek J, Bala S, Csak T, Lippai D, Kodys K, Menashy V, Barrieau M, et al. IL-1 receptor antagonist ameliorates inflammasome-dependent alcoholic steatohepatitis in mice. J Clin Invest. 2012; 122:3476–3489. [PubMed: 22945633]

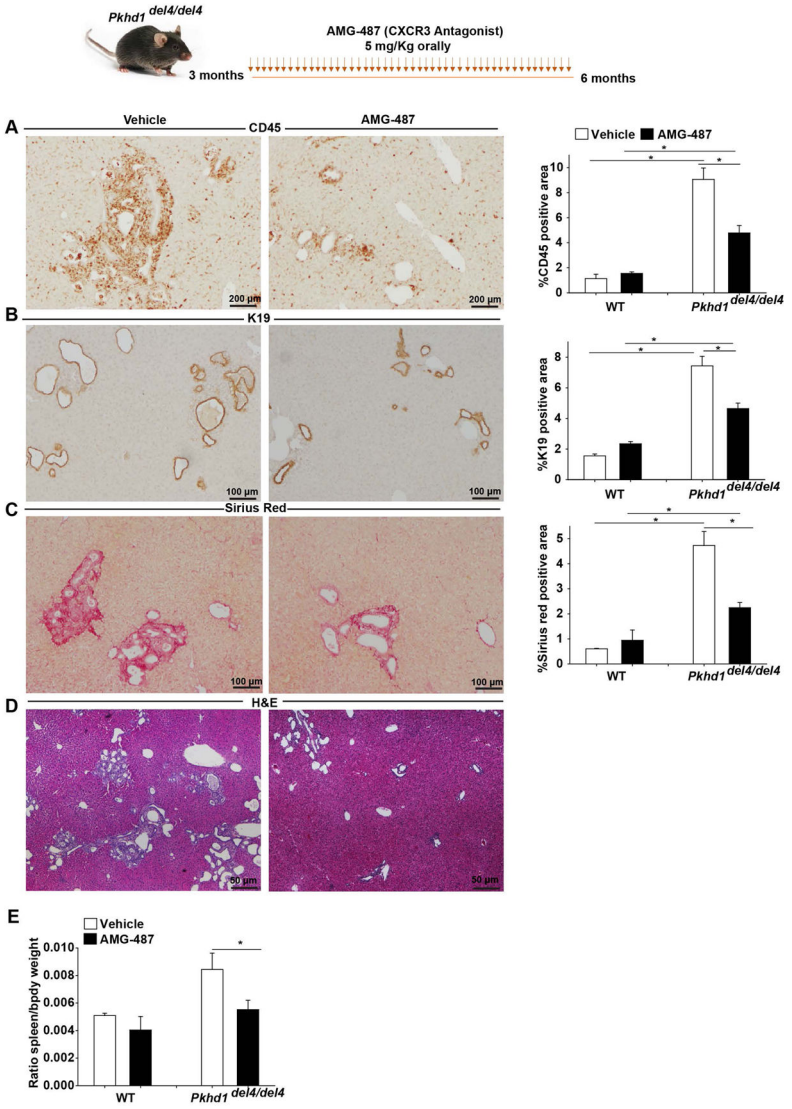

Figure 1. CXCR3 blockage slowed disease progression in *Pkhd1*$^{del4/del4}$ mice

Pkhd1$^{del4/del4}$ mice were treated with a small molecule inhibitor of CXCR3 (AMG-487, 5mg/Kg) or its vehicle orally for 3 months. AMG-487 treated mice (n=13) show reduction in: **A)** the infiltration of immune cells (CD45^{+}) as assessed by IHC for CD45 and their respective quantification. Magnification x200 **B)** the K19 positive area as assessed by IHC for K19 and their respective quantification. Magnification x100. **C)** the collagen deposition as assessed by Sirius red staining and their respective quantification. Magnification x100. **D)** Hematoxylin and Eosin (H&E) of the AMG-487 and Vehicle treated mice. Magnification x40 **E)** the splenomegaly as assessed by the ratio of spleen to body weight compared to vehicle treated mice (n=13). The quantification of CD45, K19 and Sirius red positive area was performed with image J by measuring 10 independent fields per liver specimen. (*p<0.05, ANOVA with post hoc corrections test). IHC: Immunohistochemistry, K19: Cytokeratin-19.

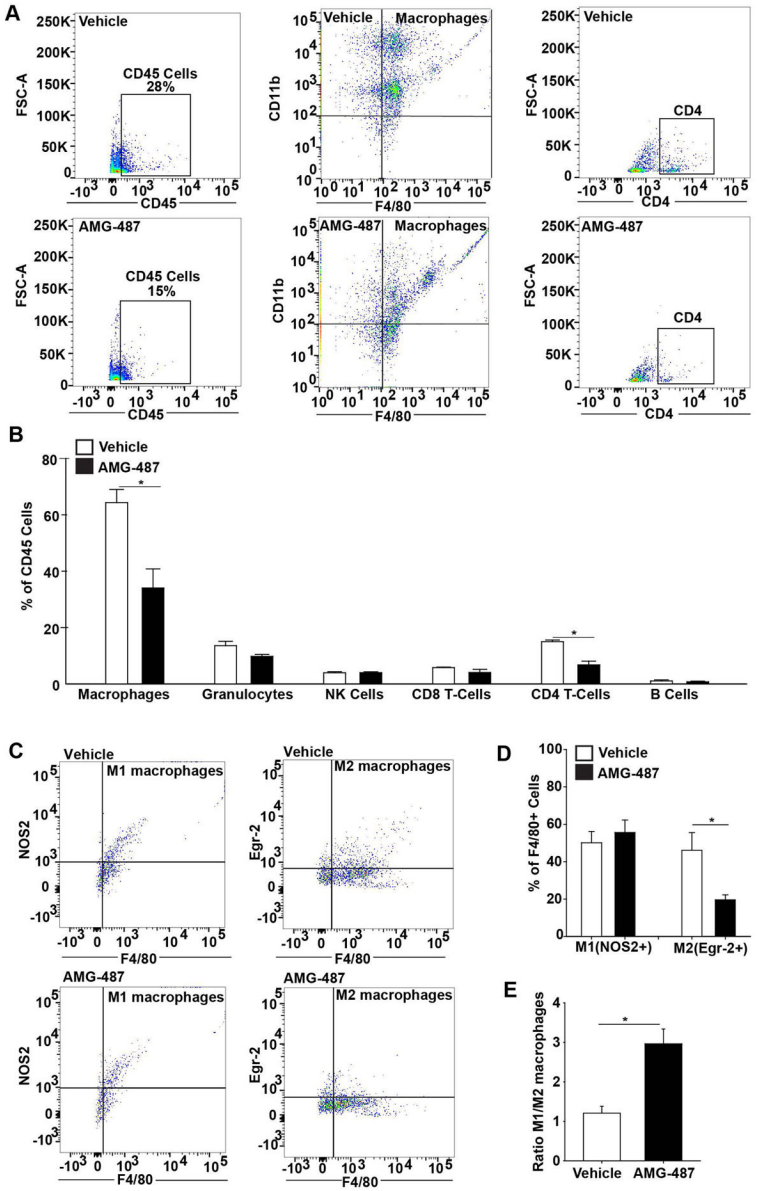

Figure 2. CXCR3 blockage reduced macrophages and T_h-cells($CD4^+$) recruitment in *Pkhd1*$^{del4/del4}$ mice

A, B) FACS analysis of whole liver for the different subpopulations of immune cells in *Pkhd1*$^{del4/del4}$ mice treated orally with a small molecule inhibitor of CXCR3 (AMG-487, 5mg/Kg) (n=3) or its vehicle (n=3) for 3 months. AMG-487 treated mice had reduced macrophages and $CD4^+$ T cells infiltration. **C, D)** FACS analysis of the whole liver in the same mice for the M1($NOS2^+F4/80^+$) and M2($Erg2^+F4/80^+$) macrophages shows reduced levels of the M2 upon CXCR3 treatment. **E)** The M1/M2 ratio is increased in AMG-487 treated *Pkhd1*$^{del4/del4}$ mice. The analysis was performed in the selected CD45 positive cells (*p<0.05, unpaired Students Ttest). NOS2: Nitric oxide synthase 2, Erg-2: Early growth response protein-2.

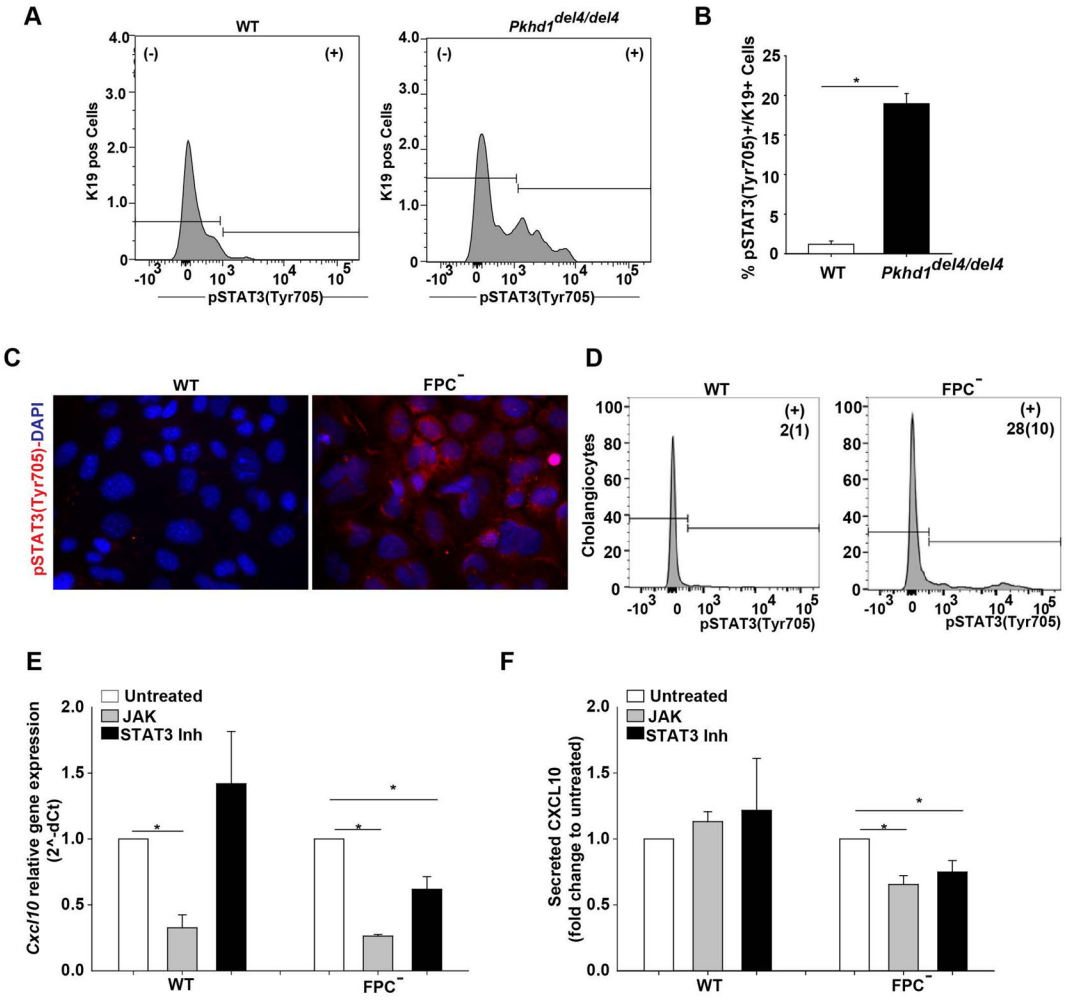

Figure 3. In FPC-defective cholangiocytes an increased pSTAT3(Tyr705) is responsible for CXCL10 production

A) FACS analysis in the liver of 3 months old WT/*Pkhd1*$^{del4/del4}$ mice shows increased number of Cholangiocytes (K19^{+}Cells) that express pSTAT3(Tyr705) in *Pkhd1*$^{del4/del4}$ (n=3) compared to WT mice (n=3). **B)** Bar graph showing the quantification of FACS analysis results. **C)** Immunocytochemistry for pSTAT3(Tyr705) (red) in WT and FPC-defective cholangiocytes (FPC^{-}) showed cytoplasmic and nuclear expression only in FPC-defective cholangiocytes. Nuclei were stained with DAPI (blue). **D)** FACS analysis for pSTAT3(Tyr705) in the cultured WT and FPC-defective cholangiocytes showed increased expression of pSTAT3(Tyr705) in FPC-defective cholangiocytes as compared to WT cells. The number in (+) fraction for pSTAT3 are mean(SD) of % pSTAT3^{+} Cholangiocytes. **E, F)** *In vitro* treatment of WT (n=7) and FPC-defective cholangiocytes (n=8) with inhibitor of JAK or STAT3 activation for 24 hours reduced *Cxcl10* gene expression as assessed by RT-PCR and CXCL10 protein levels as assessed by ELISA in the cell supernatant compared to untreated cells only in FPC-defective cholangiocytes. The results in graph E and F are presented as fold change to untreated cells and the statistics were performed with the one

sample Ttest. (*p<0.05, unpaired Students Ttest). K19: Cytokeratin-19, FPC^{-}: Fibrocystin-defective cholangiocytes.

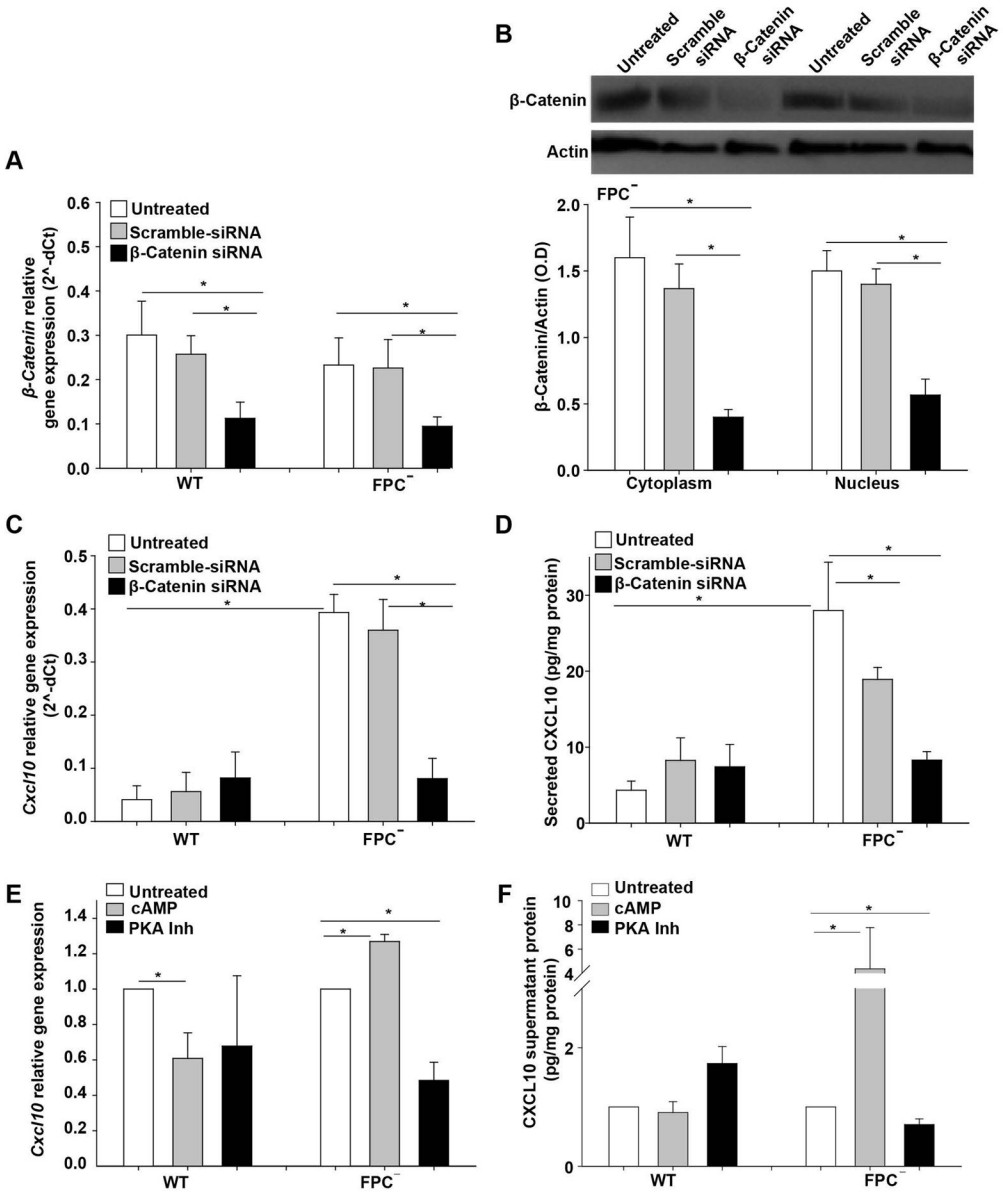

Figure 4. CXCL10 gene expression and secretion is β-Catenin and cAMP dependent

WT and FPC-defective cholangiocytes (FPC⁻) were transfected with specific siRNAs for β-Catenin or with scrambled siRNA. RNA, protein and supernatant were collected 48 hours post transfection. **A)** *β-Catenin* gene expression was reduced in WT and FPC-defective cholangiocytes transfected with the β-Catenin siRNA. **B)** β-Catenin protein expression was reduced in FPC-defective cholangiocytes transfected with the β-Catenin siRNA. **C)** *Cxcl10* gene expression was significantly reduced only in FPC-defective cholangiocytes silenced for β-Catenin. **D)** In the same way, CXCL10 protein levels measured by ELISA in cell supernatants were reduced only in FPC-defective cholangiocytes (n=6). **E, F)** WT and FPC-defective cholangiocytes (FPC⁻) were treated with cAMP or PKA inhibitor for 24 hours. *β-Catenin* gene expression and secretion was increased upon cAMP treatment and decreased

upon PKA inhibition only in FPC-defective cholangiocytes and not in WT cells (*$p<0.05$, ANOVA with post hoc corrections). FPC^{-}: Fibrocystin-defective cholangiocytes.

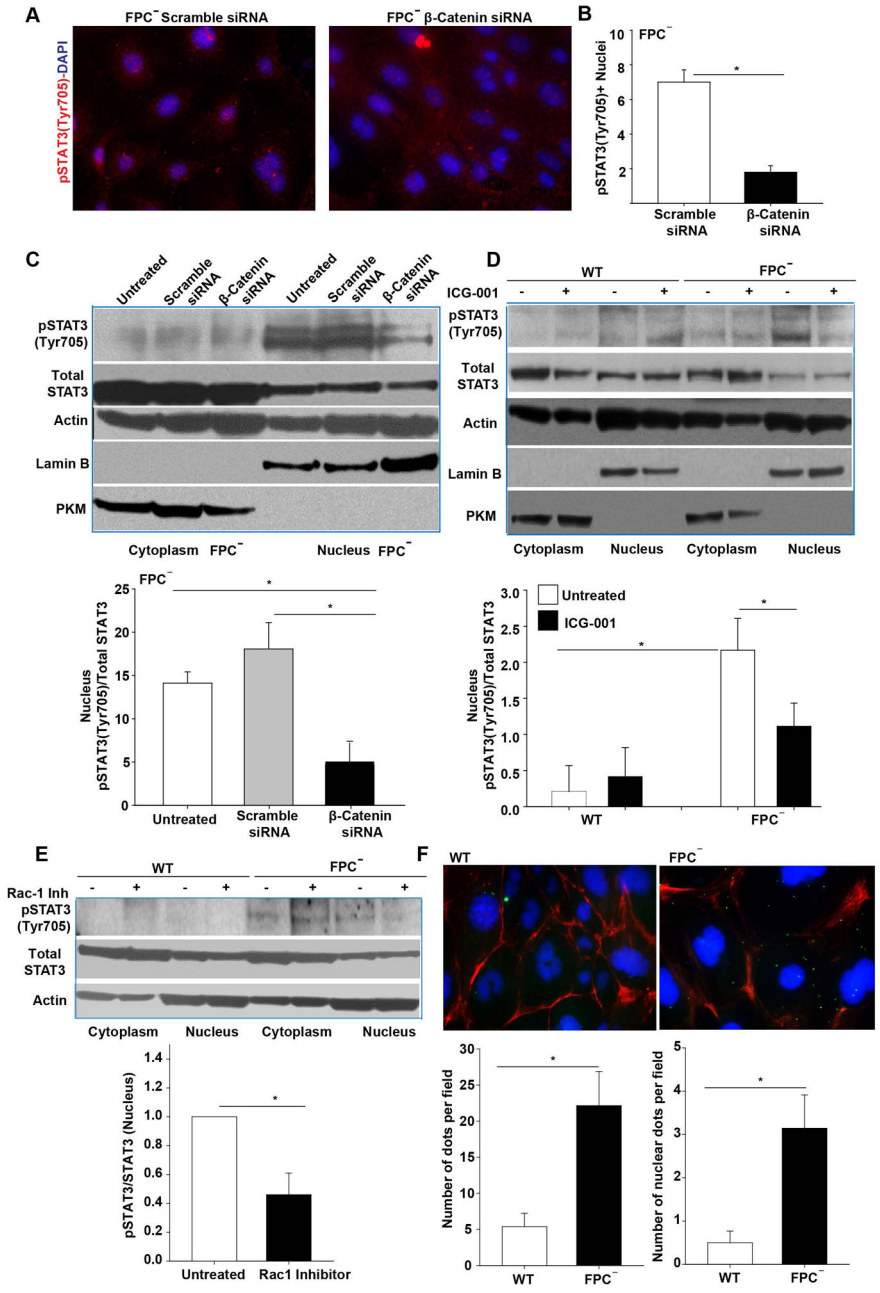

Figure 5. β-catenin silencing or inhibition blocked pSTAT3(Tyr705) nuclear translocation in FPC-defective cholangiocytes

A) Immunocytochemistry for pSTAT3(Tyr705) (red) showed reduction in its nuclear expression in FPC-defective cholangiocytes (FPC⁻) silenced for β-Catenin. Nuclei were stained with DAPI (blue). **B)** Bar graph showing the quantification of pSTAT3(Tyr705) positive nuclei from A in the FPC-defective cholangiocytes (n=3). **C)** Western blot analysis for pSTAT3(Tyr705), STAT3, actin, lamin B, and PKM in nuclear and cytoplasmic extracts of FPC-defective cholangiocytes and the respective quantification shows a reduction in nuclear pSTAT3(Tyr705) upon β-Catenin silencing (n=5). **D)** Similar results were obtained in FPC-defective cholangiocytes treated with β-Catenin inhibitor (ICG-001), (n=4). **E)**

Western blot analysis for pSTAT3(Tyr705), STAT3, lamin B and actin in nuclear and cytoplasmic extracts of FPC-defective cholangiocytes and the respective quantification showed a reduction in the nuclear expression of pSTAT3(Tyr705) upon Rac-1 inhibition (n=3). **F)** PLA assay showed an interaction between β-Catenin and pSTAT3. Quantification of dots showed that this interaction was significantly higher in FPC-defective cholangiocytes compared to WT cells (n=3). (*p<0.05, Students Ttest or ANOVA with post hoc corrections). Pan-Akt: pan-protein kinase isoform 1,2,3. FPC^{-}: Fibrocystin-defective cholangiocytes.

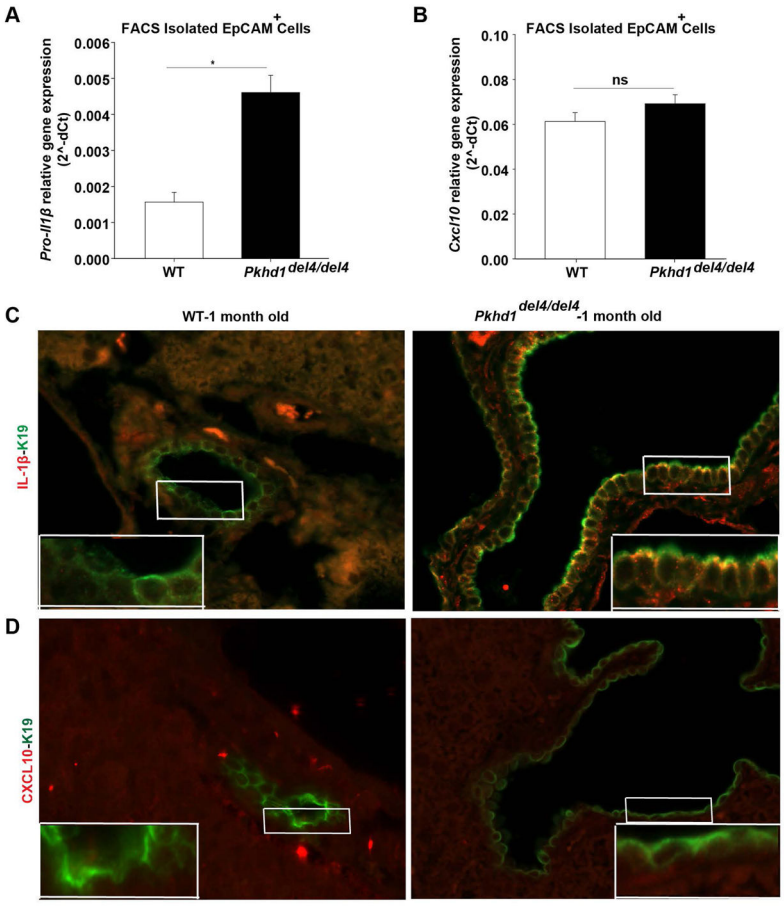

Figure 6. IL-1β is produced earlier than CXCL10 in *Pkhd1*$^{del4/del4}$ cholangiocytes *in vivo*.

A, B) Cholangiocytes (EpCAM^{+} Cells) isolation with FACS sorting from liver of 1-month-old mice. **A)** *pro-IL-1β* gene expression assessed by RT-PCR was increased whereas **B)** *Cxcl10* gene expression was unaltered in cholangiocytes isolated from 1-month-old *Pkhd1*$^{del4/del4}$ mice compared to WT mice of the same age. **C)** IL-1β (red) was expressed in cholangiocytes (K19^{+} cells, green) in liver specimens from 1-month-old *Pkhd1*$^{del4/del4}$ but not from WT mice as assessed by immunofluorescence. **D)** CXCL10 (red) was not expressed in cholangiocytes (K19^{+} cells, green) either in WT or in *Pkhd1*$^{del4/del4}$ in 1-month old mice. (*p<0.05, Students Ttest). FPC^{-}: Fibrocystin-defective cholangiocytes. K19: Cytokeratin-19.

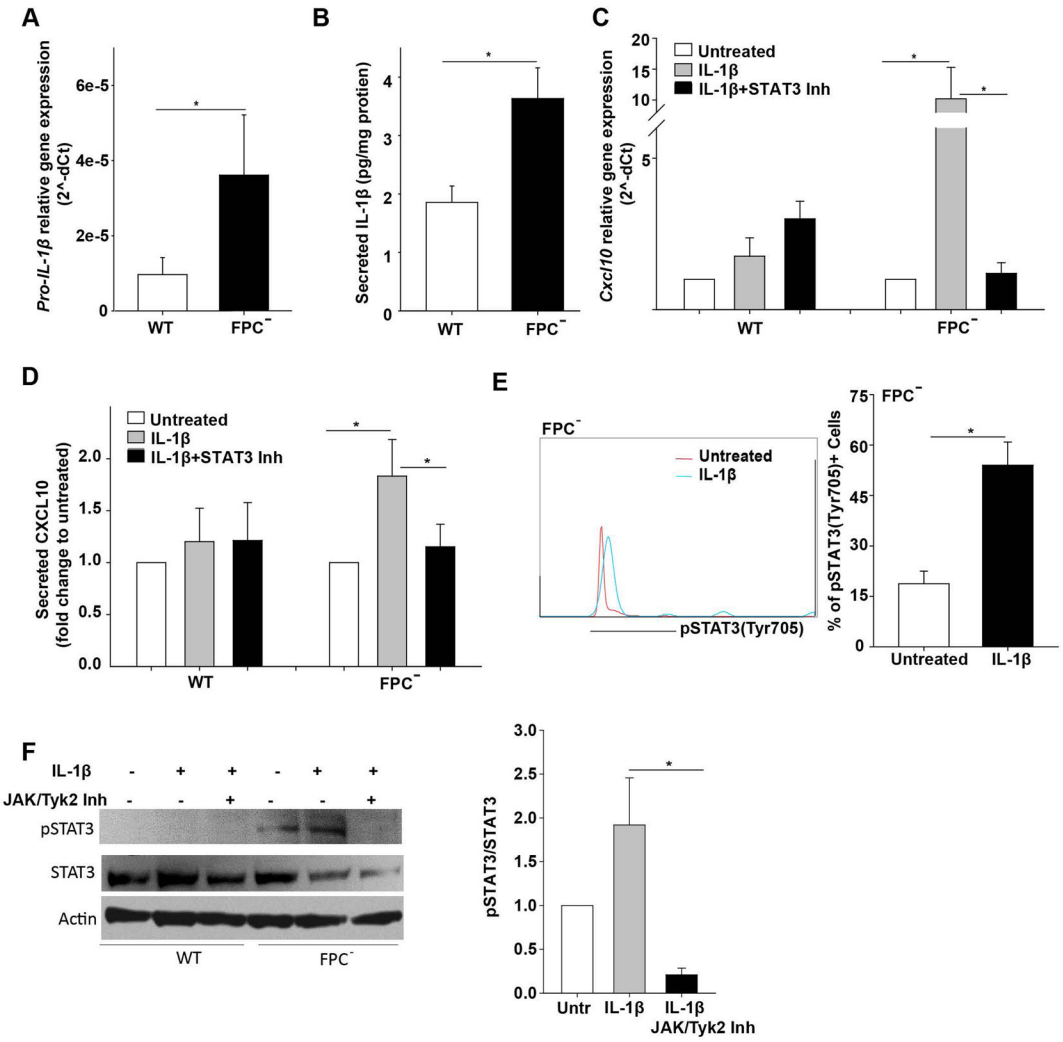

Figure 7. Increased IL-1β production from FPC-defective cholangiocytes is responsible for increased CXCL10 through JAK/STAT3 pathway

A) *Pro-IL-1β* gene expression was increased in FPC-defective cholangiocytes (FPC⁻) compared to WT cells (n=8). **B)** IL-1β protein levels measured by ELISA in cell supernatant was increased in FPC-defective cholangiocytes compared to WT cell *in vitro* (n=8). **C, D)** Treatment with STAT3 inhibitor inhibited the IL-1β-induced *Cxcl10* gene expression and CXCL10 protein levels in FPC-defective but not in WT cholangiocytes (n=8). **E)** FACS plot showed increased expression of pSTAT3(Tyr705) in FPC- defective cholangiocytes treated with IL-1β for 1 hour as compared to untreated cells and the respective quantification(n=3). **F)** Western blot of pSTAT3 and the respective quantification showing that the induction of pSTAT3 upon IL-1β treatment was abolished in the presence of JAK/Tyk2 inhibitor (n=3). The results in graph C and D are presented as fold change to untreated cells and the statistics were performed with the one sample Ttest (*p<0.05; Students Ttest). FPC⁻: Fibrocystin-defective cholangiocytes.

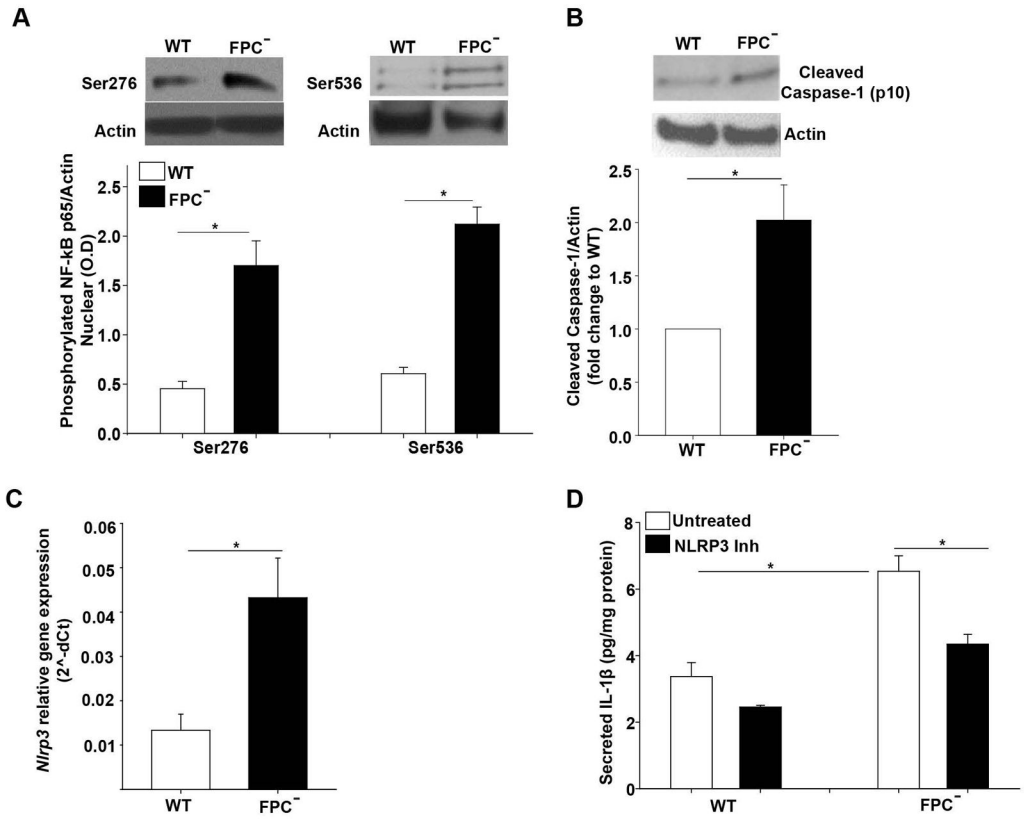

Figure 8. Inflammasome activation is increased in FPC-defective cholangiocytes and is responsible for IL-1β secretion

A) Western blot analysis for phosphorylated p65 fraction of NF-kB (Ser276 and Ser536) in nuclear cell extracts showed increased phosphorylated p65 in FPC-defective (FPC⁻) as compared to WT cholangiocytes (n=5). **B)** Similarly, cleaved caspase-1 (p10) was increased in FPC-defective cholangiocytes as compared to WT (n=6). **C)** *Nlrp3* gene expression was increased in FPC-defective cholangiocytes compared to WT (n=8). **D)** Treatment with an inhibitor of NLRP3 canonical and non-canonical activation (MCC950) decreased IL-1β protein levels in FPC-defective cholangiocytes compared to WT (n=6). (*p<0.05, Students Ttest or ANOVA with post hoc corrections). NLRP3: Nod-like receptors, pyrin domain containing 3. FPC⁻: Fibrocystin-defective cholangiocytes.